Study and Modelling of Saltwater Intrusion into Aquifers.
Proceedings 12th Saltwater Intrusion Meeting, Barcelona, Nov. 1992. CIHS.

INFLUENCE OF SEA LEVEL RISE ON A GROUNDWATER FLOW SYSTEM IN NOORD-HOLLAND, THE NETHERLANDS

G.H.P. Oude Essink, H.A. Paap, and **R.H. Boekelman**
Delft University of Technology, Faculty of Civil Engineering,
Sanitary Engineering & Water Management Group,
2628 CN Delft,
THE NETHERLANDS.

SUMMARY

In this paper, an adapted version of the two-dimensional model *MOC* is employed to simulate the influence of sea level rise on groundwater flow through a cross-section in the province Noord-Holland, The Netherlands. The investigation is focused upon several scenarios of sea level rise, some effects of human measures to counteract the impacts of sea level rise and a limited sensitivity analysis of geohydrological parameters.

Salt water intrusion into the coastal geohydrologic system already occurs independently of sea level rise, since the salinisation process is initiated by human interventions (e.g., creation of low-lying polders). However, sea level rise accelerates salt water intrusion significantly. Nevertheless, there will still be a considerable time lag of several centuries between the causes of changes and the ultimate effects on the salinisation process. The zone of influence is several kilometres, since the aquifer system has a high transmissibility. As a result, changes in seepage in low-lying polders -both quantitative and qualitative- can not be neglected. However, the impact of sea level rise can be counteracted -not entirely neutralized- by measures, though these measures will be effective only after a considerable time lag. Even so, effects of sea level rise on salt water intrusion are of the same order of magnitude as possible errors in some geohydrological parameters, such as transmissibilities and dispersivities; thus more field measurements concerning these parameters are necessary.

1. INTRODUCTION

As The Netherlands is a low-lying country, sea level rise affects water management sectors such as public and industrial water supply, ecology, agriculture and horticulture. The groundwater flow system plays an important role in the effect of sea level rise on water management. For instance, salt water will intrude into deep aquifers, volumes of freshwater lenses under sand-dunes will change and seepage in low-lying polders further inland will increase in quantity and quality. The effects of sea level rise on water management have to be determined in order to recognize the impacts on society in time and to take adequate measures.

Therefore, in this paper, the impacts of sea level rise on the groundwater flow regime in a specific cross-section perpendicular to the Dutch coast in Noord-Holland are investigated. The two-dimensional groundwater flow model MOC of Konikow & Bredehoeft (1978) of the US Geological Survey is used to assess the effect of sea level rise in the cross-section on groundwater flow and on solute transport. The model is adapted for *density differences* with documentation of Lebbe (1981, 1983) and Van der Eem (1987), and as a result, density flow in a *vertical* cross-section can be simulated.

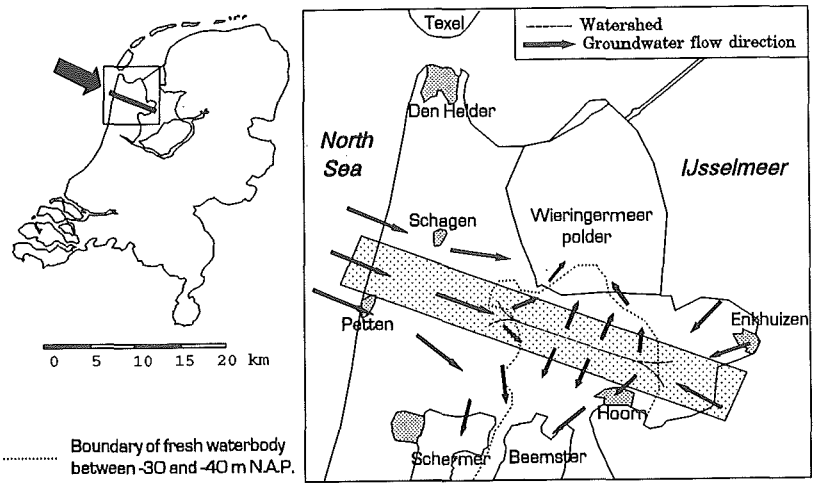

Figure 1: *The map with the cross-section in a part of the western province Noord-Holland in The Netherlands.*

Section 2 of this paper gives the present situation of the simulated cross-section. In section 3, a short description of the groundwater flow model MOC is given, relevant geohydrological parameters are summarized and the geohydrologic system is schematized and calibrated. In section 4, simulations of the geohydrologic system with different scenarios of sea level rise are discussed and changes in groundwater flow and solute transport are quantified. In section 5, the influences of some compensating human measures are investigated, such as deep-well infiltration, abstraction of saline groundwater and variation of phreatic groundwater level in polders. In section 6, the influence of some geohydrological parameters on the solute transport in the geohydrologic system is analysed. Finally, conclusions are presented.

2. PRESENT SITUATION

The cross-section is situated in the province Noord-Holland (fig. 1). This part of The Netherlands is surrounded by the North sea at the west side, and by the IJsselmeer at the east side. The IJsselmeer (former Zuider Zee) was brackish and in open connection with the North Sea till 1932. In 1932, the inlet was closed by a dam (the Afsluitdijk) and as a consequence, the former Zuider Zee became a freshwater lake: IJsselmeer.

In the central part of the cross-section the so-called fresh waterbody of Hoorn is situated (chloride concentration 200 mg/l), which extends at some places to a depth of 90 m below mean sea level. The phreatic groundwater levels of the polders along the cross-section vary from about -0.5 m *N.A.P.*[1] in the polders near the coast till about -3.1 m *N.A.P.* in the polders near the IJsselmeer. At some kilometres perpendicular to the center of the cross-section some large low-lying polder areas come across: at the north side the Wieringermeer,

[1] *N.A.P.* ('Normaal Amsterdams Peil') is the reference level in The Netherlands. *N.A.P.* roughly equals Mean Sea Level.

which is reclaimed in 1930, and at the south side the Beemster and the Schermer, reclaimed in respectively 1612 and 1635 (Schultz) [1]. These reclaimed areas affect the groundwater flow, which can be deduced from piezometric levels at several depths below *N.A.P.* (ICW) [2]. Hardly no freshwater lens is present under the sand-dunes along the Dutch coastline, since the width of the sand-dunes through this cross-section is only about one kilometre.

The evolution to the present situation in terms of solute distribution of the fresh waterbody of Hoorn is as follows (Beekman) [3].

The refreshening of the fresh waterbody of Hoorn is induced by geological and human activities since Medieval times. In the central part of the fresh waterbody, the groundwater age appears to be younger than 250 years. Since Medieval times, peat areas, which cross the area of the fresh waterbody, are subsiding due to drainage. As a consequence, the tidal channels relatively rise with respect to the peatland. Primarily, infiltration of fresh surface water took place within this complex system of tidal channels and peat areas. After reclamation of lakes, especially since the 17^{th} century, groundwater flow to the north and the south was induced. Salinisation of aquifers in the west and active refreshening in the northern area of the fresh waterbody are related to those changes in groundwater flow direction.

However, some other hypotheses such as ICW [2] and Pomper [4] suggest that the lateral extend of the fresh waterbody is the result of a forced displacement of fresh groundwater by the (Eemian) seawater intrusion from the west and the presence of less permeable layers, deposited simultaneously. These hypotheses have in common that formation of the fresh waterbody is dated at least 3000 years ago, and that ultimately the fresh waterbody will disappear.

3. SCHEMATIC OUTLINE

In this section, a short description of MOC is given. Model parameters, geometry of the cross-section and geohydrological parameters used in the reference case are summarized. Furthermore, the calibration is given for piezometric levels and flow of groundwater through the Holocene aquitard. The data of the geohydrologic schematization have been borrowed from the following sources: Paap [5], De Wilde [6], Pomper [7], Witt [8], ICW [2] and TNO [9].

3.1 Short description of MOC

The solute transport model MOC ('Method of Characteristics') from the US Geological Survey is developed by Konikow & Bredehoeft in 1978 [10]. Originally, MOC is a *horizontal* two-dimensional groundwater flow model. However, *vertical* cross-sections have to be simulated here, since the geohydrologic systems near the Dutch coast have non-uniform density distributions. The groundwater flow equation in MOC (version 3.0 of 1989, [11]) is adapted for *density differences*, see Lebbe [12], [13], Van der Eem [14] and Oude Essink [15].

Since the chloride content in groundwater is the most important negative ion and is investigated intensively, the distribution of chloride is considered to represent the salinisation process. The classification of *fresh*, *brackish* and *saline* groundwater is according to Stuyfzand [16], see table 1. The chloride concentration in the groundwater is used to determine the density of groundwater. The conversion from chloride concentration to density is as follows (equation 1):

$$\rho_i = \rho_0 * (1 + \frac{\rho_{ref} - \rho_0}{\rho_0} * \frac{C_i}{C_{ref}}) \qquad (1)$$

Type of groundwater	Chloride concentration $[mg\ Cl^-/l]$
fresh	$Cl^- <= 300$
brackish	$300 < Cl^- < 10000$
saline	$Cl^- >= 10000$

Table 1: *The classification of fresh, brackish and saline groundwater depending on the chloride concentration, after Stuyfzand.*

where ρ_i is the density of groundwater at grid cell i $[ML^{-3}]$; ρ_0 is the standard reference density, usually the density of fresh groundwater ($\rho_0 = 1000\ kg/m^3$); ρ_{ref} equals the density of saline groundwater ($\rho_{ref} = 1025\ kg/m^3$); $\frac{\rho_{ref}-\rho_0}{\rho_0}$ is the relative density difference [−] ($\frac{\rho_{ref}-\rho_0}{\rho_0} = 0.025$); C_i is the chloride concentration in grid cell i $[mg\ Cl^-/l]$; and C_{ref} is the reference chloride concentration for which saline groundwater equals a density of 1025 kg/m^3 ($C_{ref} = 18630\ mg\ Cl^-/l$).

3.2 The reference case

(a) Model parameters

Total number of grid cells is 5162: in horizontal direction 178 and in vertical direction 29 grid cells. Each grid cell is 250 m long and 10 m high. The total cross-section is 44500 m long and 290 m high. Each grid cell has sixteen particles representing the chloride concentration . The convergence criterion TOL for the (iterative) calculation of the groundwater flow equation is 10^{-5} $feet^2$. After every groundwater flow simulation step of *one* year, the groundwater flow equation is calculated again. During this step, the velocity field remains constant. In most cases through this cross-section the *chemical time step*[3], which determines the solute transport, equals the time step of the groundwater flow. The maximum distance CELDIS across one grid cell, in which a particle is allowed to move during one *chemical time step*, is set to 0.5 (as a fraction of the grid cell).

(b) Geohydrological parameters

In fig. 2 the geometry, hydraulic conductivities of aquifers and hydraulic resistances of aquitards in the cross-section are given. Fig. 3 shows the present chloride distribution of the cross-section, derived from Witt [8] and ICW [2].

The longitudinal dispersivity α_L is initially set to a small value: 0.02 m (Kooiman) [17]. A limited sensitivity analysis on this parameter is executed later in this paper. The ratio transversal to longitudinal dispersivity is set to 0.1 [−], while the anisotropy factor (the ratio vertical and horizontal hydraulic conductivity) is also 0.1 [−]. The effective porosity is 0.35 [−] and the specific storativity S_s is set to zero.

(c) Boundary conditions

The phreatic groundwater levels in the polders at the horizontal upper boundary, derived from De Wilde [6], are kept constant. The natural groundwater recharge at the sand-dunes is 360 mm per year. A *constant piezometric level* boundary is introduced for both the seaside as the lake side boundary, where the situation is supposed to be *hydrostatic* [12], [15]. The

[2]MOC uses the Anglo-Saxon system.

[3]A *chemical time step* is the time increment in which a particle is moved over a distance proportional to the length of that time increment and the velocity at the position of that particle.

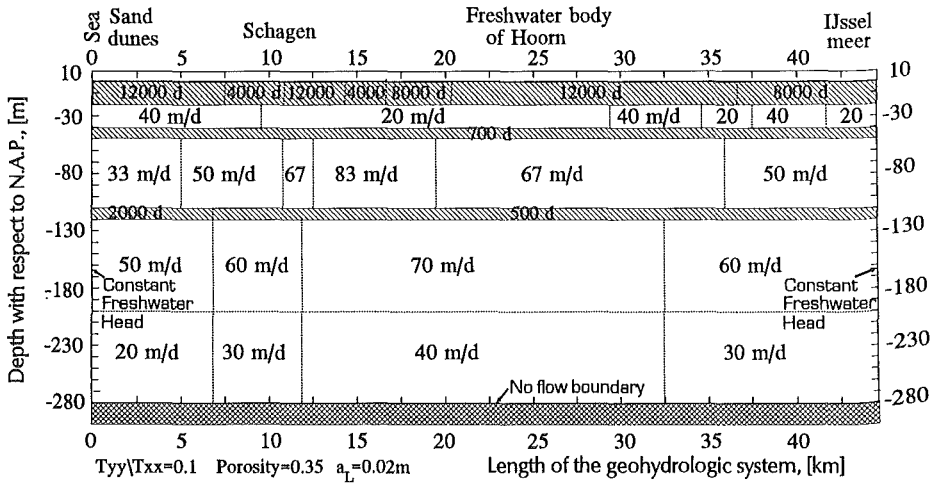

Figure 2: *Geohydrological parameters in the cross-section through Noord-Holland.*

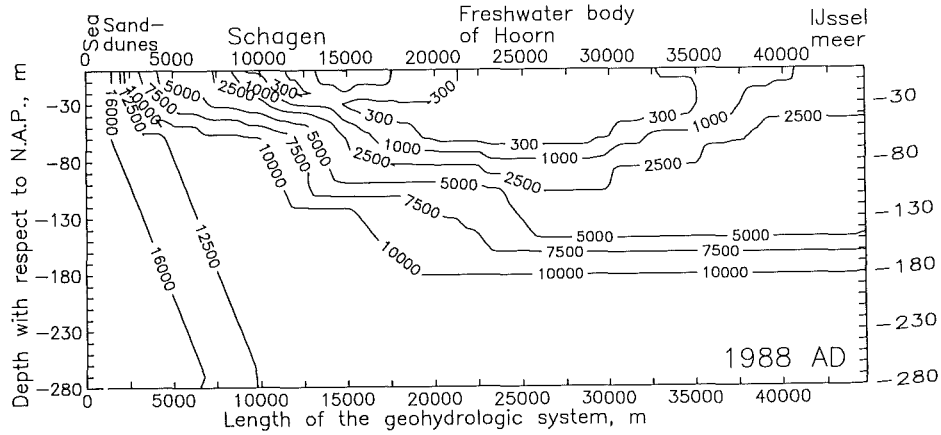

Figure 3: *The initial chloride distribution at 1988.*

piezometric level at the North Sea side is at present -0.08 m *N.A.P.* and at the IJsselmeer side -0.30 m *N.A.P.*

(d) Groundwater flow perpendicular to cross-section

As mentioned above, deep low-lying polder areas at the north (Wieringermeer) and the south (Beemster and Schermer) induce groundwater flow perpendicular to the cross-section (fig. 1). So groundwater flow perpendicular to the cross-section has to be introduced also. Therefore, the reference case simulates also a *groundwater discharge* out of the geohydrologic system at the central part of the cross-section, in order to achieve the effect of deep polders.

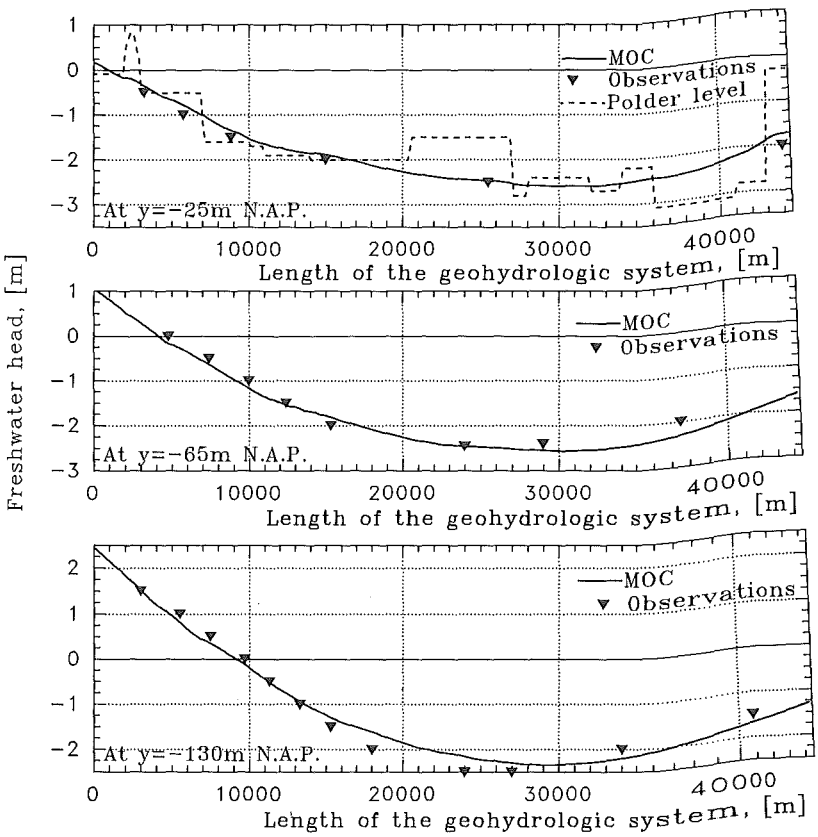

Figure 4: *The freshwater heads at -25, -65 and -130 m N.A.P., with respect to N.A.P. A comparison with some observations of the (corrected) piezometric levels, borrowed from ICW.*

3.3 Calibration

The present situation is calibrated with freshwater heads and groundwater flow through the Holocene aquitard.

(a) Piezometric levels relative to N.A.P.

Fig. 4 show the freshwater heads at -25 m, -65 m and -130 m *N.A.P.* calculated with MOC compared with observed piezometric levels (ICW) [2]. These observed piezometric levels are corrected in the vertical direction for deviation of the density of the groundwater in an observation well from the standard density ρ_0=1000 kg/m^3. The (corrected) observed piezometric levels differ only some decimetres from the freshwater heads.

(b) Groundwater flow through the Holocene aquitard

Fig. 5 gives the difference in calculated and observed piezometric level between phreatic

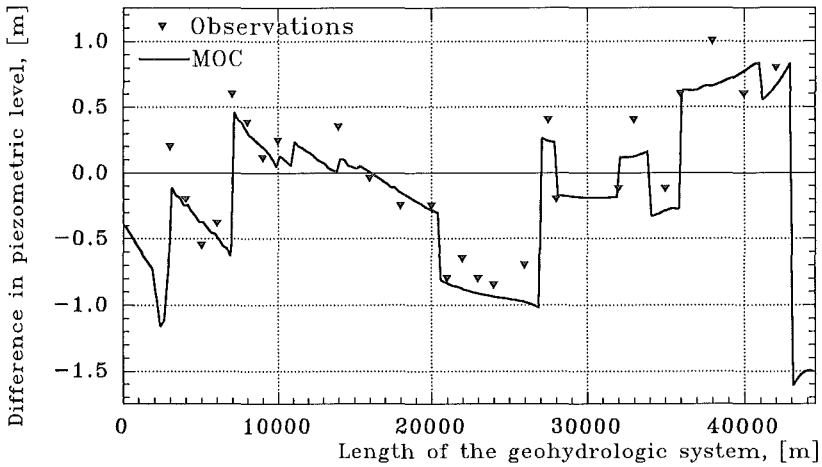

Figure 5: *The difference in piezometric level between phreatic groundwater level and piezometric level at -25 m N.A.P. in the cross-section for both calculation and observations.*

groundwater level (here *polder level*) and piezometric level at -25 m *N.A.P.* (ICW) [2]. These figures can be considered to represent seepage and infiltration values.

Observed averaged seepage and infiltration rates through the Holocene aquitard are determined by means of water balances over specific subareas. The rates for both calculated and observed values are almost everywhere smaller than 0.15 mm per day, due to the high hydraulic resistance of the Holocene aquitard (see fig. 2).

4. RESULTS OF SIMULATIONS

In this section the simulations of the geohydrologic system for the next millennium are discussed. Several scenarios of rates of sea level rise are imposed to estimate changes in groundwater flow and solute transport.

4.1 Scenarios of sea level rise

There are many prognoses of future sea level rise. Thus, in this paper six scenarios of rates of sea level rise are imposed at the seaside boundary of the geohydrologic system for a time period of 1000 years: (a) no sea level rise; (b) sea level *fall* of 60 cm per century; (c) sea level rise with a *natural trend* of 15 cm per century; (d) sea level rise of 60 cm per century, according to the IPCC[4]; (e) sea level rise of 100 cm per century; and (f) an *extreme* sea level rise of 150 cm per century.

The sea level rises are imposed as elevations[5] of freshwater head at the seaside boundary every 25 years and from the year 2013 AD on. Since a relative long time period is simulated, many processes that affect the geohydrologic system should be taken into account.

[4]The Working Group 1 of the Intergovernmental Panel on Climate Change (IPCC) has in 1990 as the best estimate under the IPCC Business-as-Usual emission scenario a global mean sea level rise of about 60 cm over the next century with an uncertainty range of 30 to 100 cm per century.

[5]Van der Eem introduced in MOC a procedure, in which during so-called pumpingperiods changes in freshwater heads can be implemented.

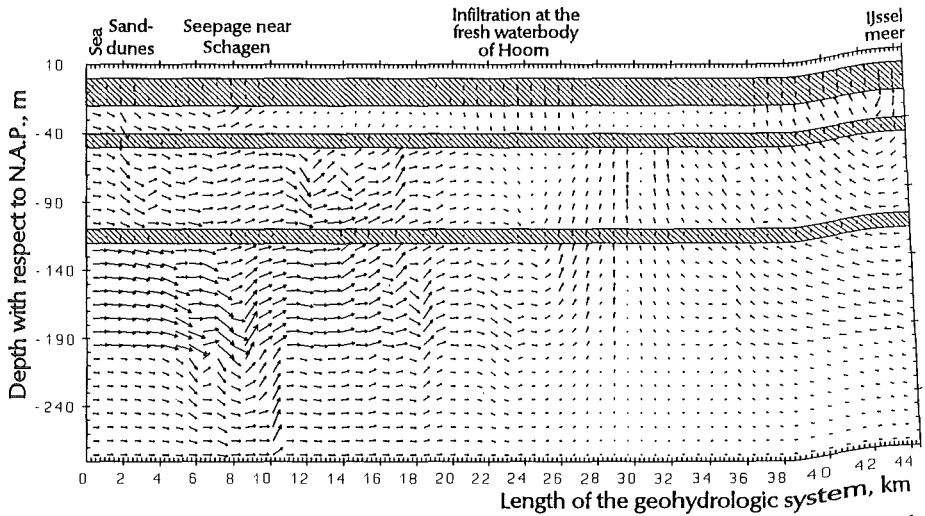

Figure 6: *The velocity field of entire geohydrologic system. An arrow corresponds to the displacement of a groundwater particle during 50 years. The velocity in the center of every third horizontal grid cell is displayed.*

Some of these processes are: hydrological changes in natural groundwater recharge (e.g., less precipitation, more evapotranspiration due to climatic change); land-subsidence; changes in morphology of shorelines; and processes induced by human interventions (e.g., reclamation of new land in sea in front of the coast and possibly sand-suppletion in coastal zones and sand-dune areas to counteract retreat of shoreline). However, the reference case is simulated with constant phreatic groundwater levels in the polders and a natural groundwater recharge in the phreatic aquifer at the sand-dune area of 360 mm per year.

4.2 Groundwater flow in the geohydrologic system

(a) Velocity field

Fig. 6 gives the present velocity field through the geohydrologic system. The length of the arrow represents the displacement of a groundwater particle during 50 years, if the velocity field would be constant during that time. As can be seen, a strong salt water intrusion is present in the deepest aquifer, in which the greatest intrusion is in that part of the aquifer where the hydraulic conductivity is the greatest. Vertical velocity dominates in the resistance layers. At the fresh waterbody of Hoorn, a downward groundwater flow through the Holocene aquitard occurs, while in deep polders groundwater flows upward, such as in the polder area near Schagen. The figure shows that the velocities in the aquifers fluctuate at some places in vertical direction, which is the result of numerical instability (see Oude Essink) [15].

(b) Waterbalances of the geohydrologic system

The waterbalances of the geohydrologic system are calculated over the flow boundaries: the seaside and the lake side boundaries and the upper boundary at the Holocene aquitard. The total in- and outflow of water is derived for a width of *one metre* perpendicular to the cross-section parallel to the coast. Two striking features of the groundwater flow are:

Case	Depth of aquifer in m with respect to *N.A.P.*	Reference case	No deep polders (Wieringermeer, Beemster & Schermer)	No deep polders & polder levels at *N.A.P.*	Polder levels at *N.A.P.*	No density differences
Salt water intrusion, $[m^3\ m^{-1}\ yr^{-1}]$						
aquifer 1	-20 to -40	55.4	44.2	7.9	19.1	42.4
aquifer 2	-50 to -110	176.4	146.9	53.0	82.4	112.1
aquifer 3	-120 to -280	622.5	533.5	270.5	359.5	333.6
Seepage in polder area near Schagen [between 7.25-16.0 km] in $m^3\ m^{-1}\ yr^{-1}$.						
(Seep. is positive: +)		81.4	348.5	56.0	-211.1	10.1
Infiltration at waterbody of Hoorn [between 16.0-27.0 km] in $m^3\ m^{-1}\ yr^{-1}$.						
(Inf. is negative: -)		-215.2	178.8	67.6	-326.3	-299.4

Table 2: *Flow of water masses at the seaside boundary through the three aquifers and through the Holocene aquitard, in m^3 per metre width per year for several situation.*

- salt water intrusion
  Table 2 gives the flow of water masses of some situations at the seaside and through the Holocene aquitard in m^3 per metre width per year at some specific places. The polders in the cross-section and the deep polder areas (the Wieringermeer, the Beemster and the Schermer) have strong influences on salt water intrusion in the aquifers. If no deep polders are present, salt water intrusion will be a bit less. However, salt water intrusion is more initiated by the present levels of the polders *in* the cross-section than by the deep polders at some kilometres distance perpendicular to the cross-section. If no density differences are taken into account, salt water intrusion will be much smaller than in the reference case.

- groundwater flow through the Holocene aquitard
  If no deep polders were present, the fresh waterbody of Hoorn would diminish very quickly due to strong seepage quantities. If the levels of the polders in the cross-section were at *N.A.P.*, a strong infiltration would occur in the polder area near Schagen, instead of seepage as in the reference case.

  Fig. 7 shows the upward flow (seepage is positive) and downward flow (infiltration) through the Holocene aquitard at -15 m *N.A.P.* in the year 2088 for different scenarios of sea level rise. It can be seen that infiltration in the polder area near the seaside (between about 3 and 7 km) will change into seepage due to sea level rise. The seepage in the polder area, that is situated near the IJsselmeer (between about 36 and 43 km), is already strong due to a low phreatic groundwater level and will hardly change due to sea level rise.

(c) Freshwater head distribution

Fig. 8 gives the present freshwater head distribution calculated with MOC. This freshwater head is corrected for salinity. A *hydrostatic* situation occurs at both the seaside and the lake side boundary. The freshwater head in the geohydrologic system at the fresh waterbody of Hoorn is low compared to the phreatic groundwater level above the Holocene aquitard, that is situated between 0 and -20 m *N.A.P.* Therefore, natural groundwater recharge (infiltration) occurs in that area.

The time lag of the rise in freshwater head in the geohydrologic system due to sea level rise can be supposed to be instantaneous, compared to the time lag of the change in solute

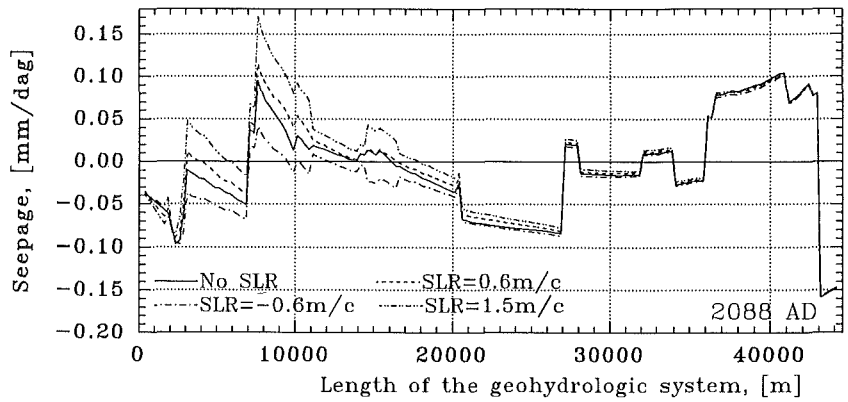

Figure 7: *The infiltration and seepage intensities through the Holocene aquitard for the year 2088. Comparison of different scenarios of sea level rise.*

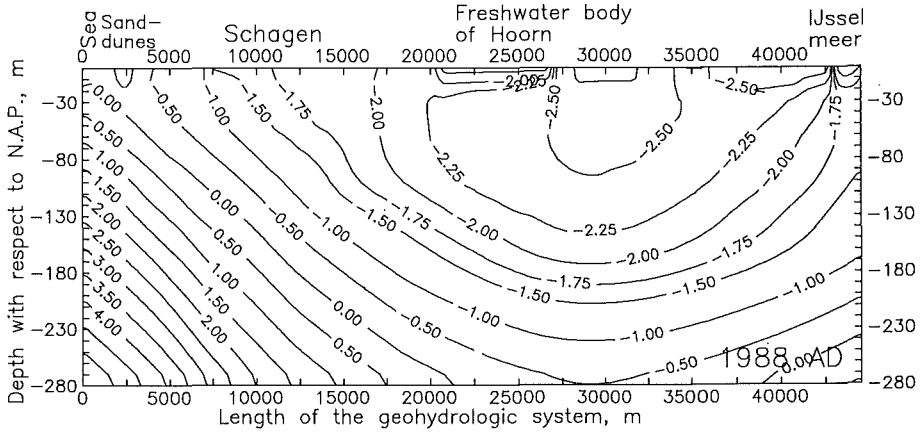

Figure 8: *The present freshwater head distribution of the geohydrologic system for the cross-section through Noord-Holland, calculated with MOC.*

distribution. Fig. 9 gives the difference in freshwater head at -25 m *N.A.P.* in the year 2088 for different scenarios of sea level rise. Since in all cases the lake side boundary is a *constant head* boundary, the freshwater head rise at -25 m *N.A.P.* and 44.5 km from the seaside is equal to zero. The zone of influence of sea level rise is quite a few kilometres which is mainly due to high transmissibilities of the aquifers. For instance, at 10 km inland of the seaside boundary, a freshwater head rise of about 25 % of the rise in sea level is still present.

4.3 Solute transport in the geohydrologic system

(a) Salt water intrusion

Fig. 10 shows the salt water intrusion during the next millennium for the reference case. As

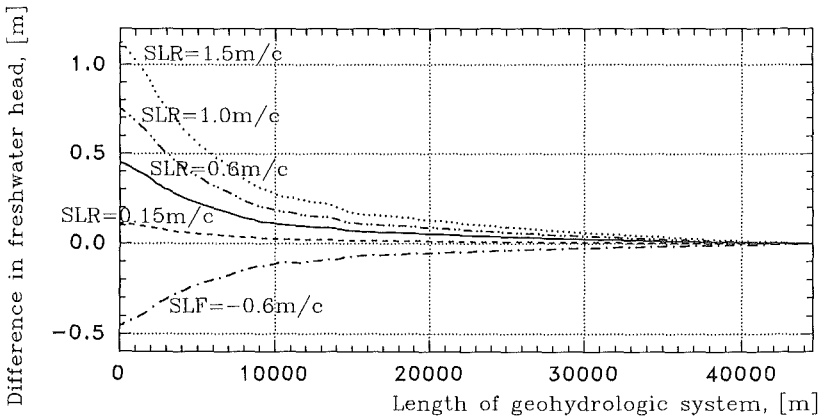

Figure 9: *The difference in freshwater head at -25 m N.A.P. in the year 2088 for different scenarios of sea level rise.*

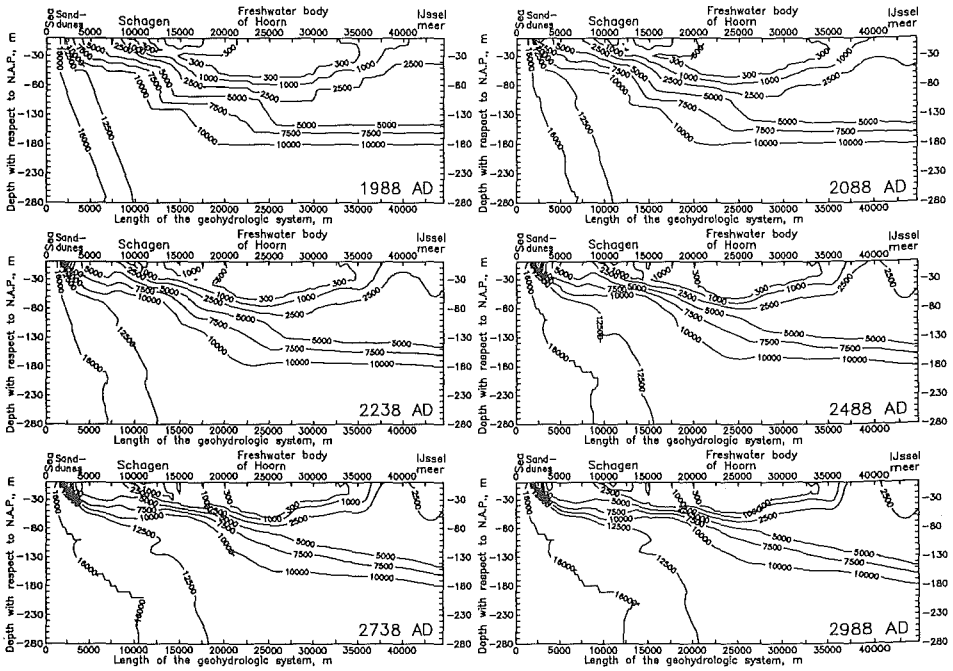

Figure 10: *The salt water intrusion in the geohydrologic system at different points in time for the reference case: no sea level rise.*

can be seen, a strong salt water intrusion occurs into the deep aquifers, but this salinisation is very slow. The new dynamic equilibrium is still not reached after one millennium. The

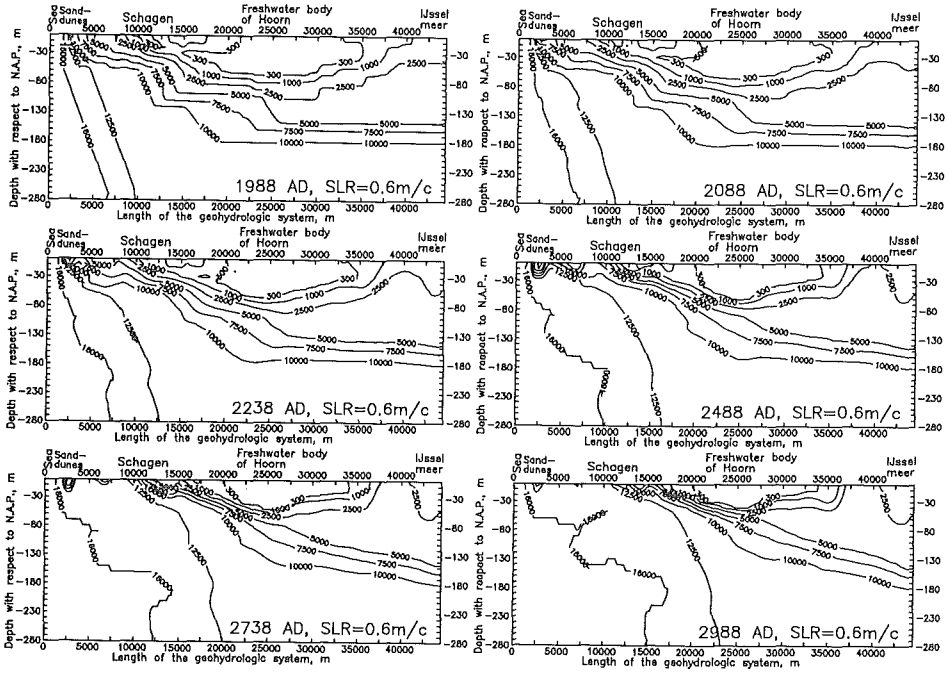

Figure 11: *The salt water intrusion in the geohydrologic system at different points in time. A constant rate of sea level rise of 0.6 m per century is imposed.*

fresh waterbody remains during the coming centuries, but the volume of fresh groundwater reduces a little. The seepage of the polder area that is situated along the IJsselmeer will contain more solute for the coming centuries.

Fig. 11 shows the salt water intrusion during the next millennium for the case with a sea level rise of 0.6 m per century. As can be seen, the fresh waterbody of Hoorn will diminish. Saline groundwater displaces brackish groundwater in the upper aquifers and aquitards at the first kilometres from the coastline. Consequently, the seepage through the Holocene aquitard in that area is saline.

In fig. 12, the salt water intrusion in the geohydrologic system is given for the year 2488 for different scenarios of sea level rise. As can be seen, it depends on the rate of sea level rise whether or not the area between the sand-dunes and Schagen contains brackish or saline groundwater. In case of sea level fall, even fresh groundwater will occur near Schagen.

Fig. 13 gives the salt water intrusion in the deep aquifer between -120 m and -280 m *N.A.P.* in m^3 per metre width per year during the next millennium at the seaside boundary for different scenarios of sea level rise. The figure shows that increase in salt water intrusion at the boundary is nearly proportional to sea level rise. Without sea level rise, salt water intrusion remains nearly constant. Meanwhile, for sea level fall of -0.6 m per century, salt water intrusion in the deep aquifer will stop at about the 26^{th} century and will change into groundwater outflow from the geohydrologic system towards the sea. If the water level in lake IJsselmeer rises with the same rate as the sea (so 0.6 m per century), salt water intrusion at

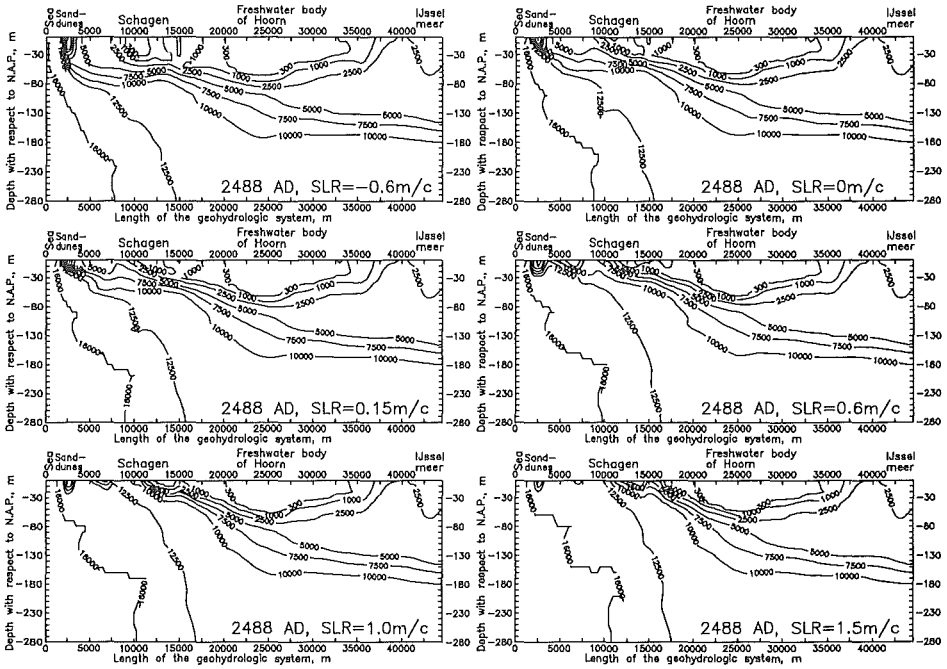

Figure 12: *The salt water intrusion in the geohydrologic system for the year 2488 for different scenarios of sea level rise.*

the seaside will be somewhat smaller compared to the reference case, since then the gradient in piezometric level in the geohydrologic system will be smaller also.

(b) Volume distribution of fresh, brackish and saline groundwater

The change in solute distribution in the geohydrologic system can be quantified by calculating the volume percentages of fresh, brackish and saline groundwater, making use of the chloride distribution and the classification of groundwater according to Stuyfzand [16] (table 1). The volume percentages are calculated for the total geohydrologic system which is bounded in horizontal direction between x=0 m and x=44500 m and in vertical direction between y=0 and y=-280 m *N.A.P.*

Fig. 14 shows the changes in volume distributions (in percentages) of fresh, brackish and saline groundwater due to sea level rise. Some striking differences are:

- if no sea level rise is imposed, salinisation of the geohydrologic system clearly takes place the coming centuries, compared to the situation at the year 1988. Both the fresh and brackish groundwater volumes in the geohydrologic system decrease a few percents the coming centuries. On the other hand, the saline fraction increases, since the polders induce salt water intrusion from the seaside,

- even with a fall in sea level, salinisation of the geohydrologic system will occur the coming centuries. Moreover, the volume of fresh groundwater would decrease also.

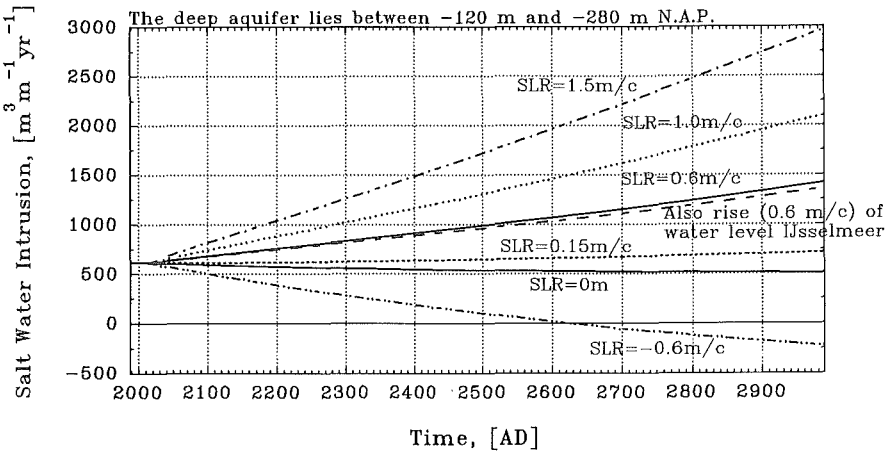

Figure 13: *The salt water intrusion in the geohydrologic system at the seaside in the deep aquifer between -120 and -280 m N.A.P. for several scenarios of sea level rise.*

However, after some more centuries, the groundwater flow near the coast will alter in direction and the geohydrologic system will contain more fresh groundwater than in the reference case,

- eventually, sea level changes will strongly affect the distribution of fresh, brackish and saline groundwater in this geohydrologic system near the coast. However, no dynamic equilibrium of the volume distribution will be reached the next millennium in this cross-section. In 2088, the differences in volume distribution between the case without and the cases with rates of sea level rise (and fall) can still be neglected. Only after some more centuries, the differences in volumes become significant.

(c) Chloride concentration in the polder area near Schagen

In fig. 15, the mean chloride concentration[6] over the polder area near Schagen in the Holocene aquitard at -15 m *N.A.P.* is given as a function of time for several scenarios of sea level rise. Only after some centuries, the differences in scenarios of sea level rise can be quantified. In cases with high rates of sea level rise, the mean chloride concentration in the Holocene aquitard increases rapidly to saline values.

Fig. 16 shows for different scenarios of sea level rise the chloride load[7] in the polder area near Schagen in ton per metre width per year. It can be seen that high rates of sea level rise generate high chloride loads in the polder area within some centuries.

(d) Summary: changes in 2088 due to sea level rise

In table 3, changes due to sea level rise of some parameters of the geohydrologic system are summarized for the year 2088, as most interest is focused on changes for the next century.

[6]Mean chloride concentration is determined here by averaging the chloride concentrations in the Holocene aquitard at -15 m *N.A.P.* over the total length of the polder area.

[7]Chloride load through the Holocene aquitard at -15 m *N.A.P.* is derived here from computed chloride concentrations and seepage or infiltration rates.

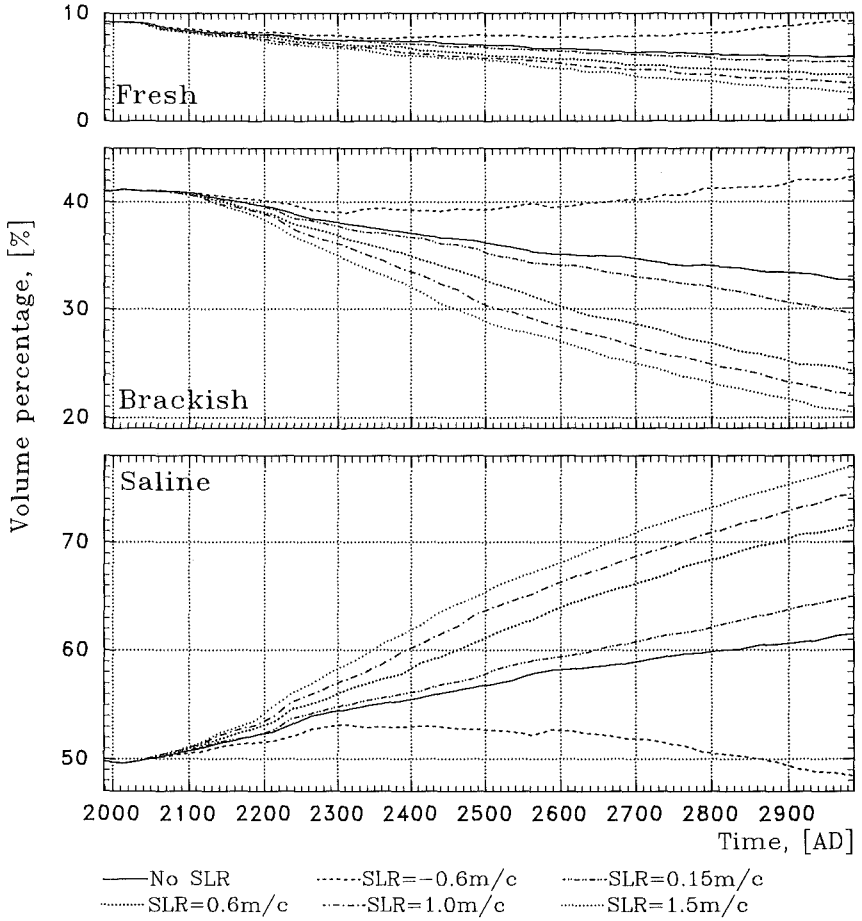

Figure 14: *The volume percentages of fresh, brackish and saline groundwater in the total geohydrologic system during the next millennium for different scenarios of sea level rise.*

In general, the differences are small the next century. The decrease in salt water intrusion in time (from 622.5 to 597.6 $m^3m^{-1}yr^{-1}$) for no sea level rise is the result of changes in chloride distribution.

5. COMPENSATING MEASURES

The following human measures are simulated to compensate the effect of the sea level rise on the geohydrologic system: (a) abstraction of saline groundwater; (b) deep-well infiltration of fresh surface water; and (c) variation of phreatic groundwater levels in the polders.

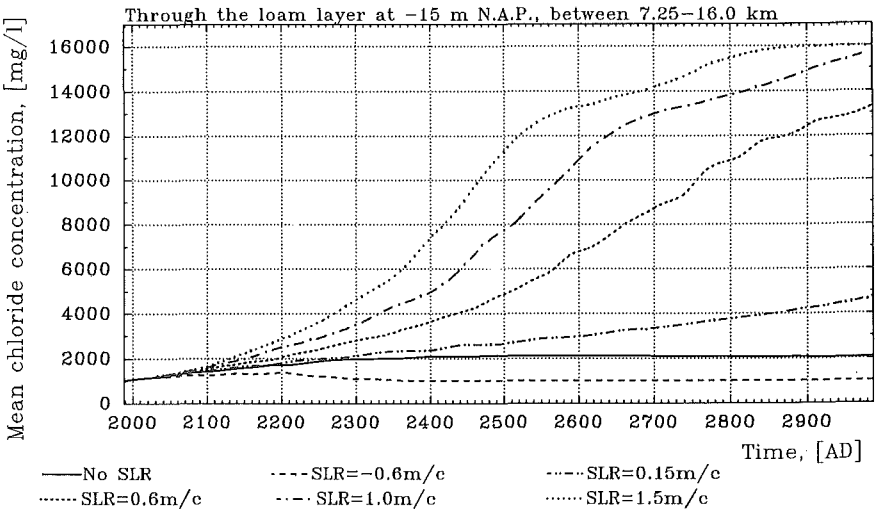

Figure 15: *The mean chloride concentration in the polder area near Schagen in the Holocene aquitard for different scenarios of sea level rise.*

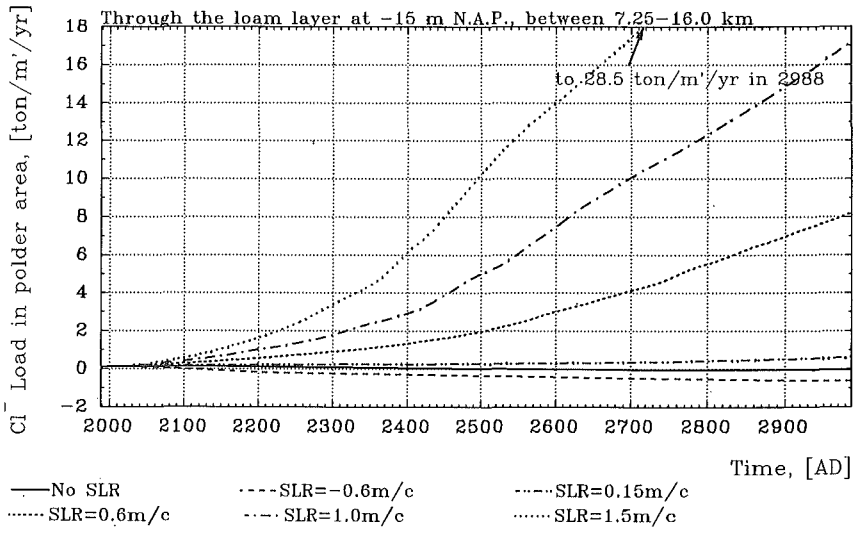

Figure 16: *The chloride load in ton per metre width per year at the polder near Schagen through the Holocene aquitard for different scenarios of sea level rise.*

Sea level rise	Year	Salt Water Intrusion	Schagen polder area [7250-16000 m]			Volumes in total system		
			Seepage	Mean Cl^-	Cl^- load	fresh	brackish	saline
[m/c]	[AD]	$[m^3m^{-1}yr^{-1}]$	$[m^3m^{-1}yr^{-1}]$	$[m^3m^{-1}yr^{-1}]$	$[m^3m^{-1}yr^{-1}]$	[%]	[%]	[%]
0	1988	622.5	-81.5	1037	0.122	9.20	40.99	49.81
-0.6	2088	519.7	2.6	1280	0.033	8.58	41.99	50.43
0	2088	597.6	-56.4	1406	0.148	8.41	40.97	50.62
0.15	2088	617.1	-71.3	1412	0.177	8.41	40.97	50.62
0.6	2088	675.2	-115.6	1468	0.277	8.35	40.88	50.77
1.0	2088	727.1	-155.0	1520	0.375	8.35	40.82	50.83
1.5	2088	792.9	-204.6	1563	0.497	8.39	40.78	50.93

Table 3: *The influence of different scenarios of sea level rise on some parameters in the geohydrologic system in the year 2088.*

The effects of human measures are quantified by comparing the simulations to the reference case for chloride load in the polder area near Schagen and for volume distribution of fresh, brackish and saline groundwater. The results of only a few different abstractions and infiltrations rates are discussed, followed by some variations in phreatic groundwater levels.

5.1 Abstraction and deep-well infiltration

Fig. 17 shows the influence of six wells with an abstraction or deep-well infiltration on the chloride load in the polder area near Schagen. The reference rate of the abstraction of groundwater or infiltration of surface water is 73.3 m^3 per metre width per year each well[8]. The rate of sea level rise is 0.6 m per century. The cases with different positions of the wells are:

- Horizontal **position 1** of the six wells: all at y=-95 m *N.A.P.* and in horizontal direction at 9875 m, 11125 m, 12375 m, 13625 m, 14875 m and 16125 m.
- Vertical **position 2** of the six wells: all at x=3625 m and in vertical direction at -55 m, -65 m, -75 m, -85 m, -95 m and -105 m *N.A.P.*

Groundwater abstraction retards groundwater flow in the direction of polder areas. Saline groundwater is removed out the geohydrologic system effectively. As a result, saline groundwater abstraction lowers chloride load in the polder areas (fig. 17).

Deep-well infiltration creates an extra strong groundwater flow in the geohydrologic system and raises seepage in the polder area near Schagen. Infiltrated fresh surface water will push brackish groundwater, occurring in the geohydrologic system, into the direction of the Holocene aquitard. Consequently, seepage has a higher chloride concentration and for the coming centuries chloride load will increase. However, the advantage of deep-well infiltration is that it creates a light brackishwater lens, and one day groundwater can be abstracted for domestic or industrial purposes from this light brackishwater lens.

The position of abstraction or deep-well infiltration wells in the geohydrologic system is rather important. Obviously, the wells must be situated near the seaside of the geohydrologic system, where the largest impact of sea level rise will be noticed. However, strong abstraction of saline groundwater near the coast will also enlarge salt water intrusion. Therefore, an optimum scheme of position and number of wells should be derived at a later stage.

Both abstracting groundwater and infiltrating surface water decreases the saline groundwater fraction, compared to the reference case. However, cases with deep-well infiltration

[8]As a vertical cross-section is simulated, the quantities are expressed in m^3 *per metre width* per year. The rate of all wells together equals for instance infiltration in a canal of about 0.44 million m^3 per year over a length of *one kilometre*.

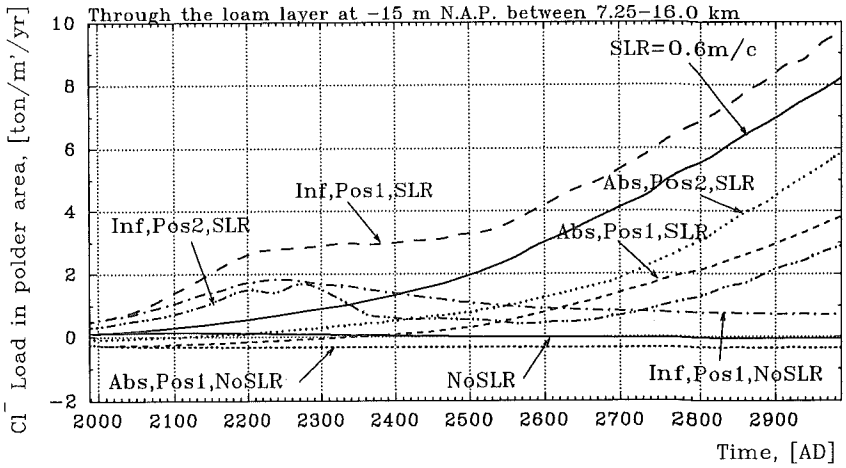

Figure 17: *The chloride load in ton per metre width per year at the polder area near Schagen through the Holocene aquitard for two different positions of the wells. The reference rate of the abstraction or infiltration is 73.3 m^3 per metre width per year each well.*

create a larger brackish zone compared to both the reference case as well as to cases with groundwater abstraction. Furthermore, if sea level rises, the fresh groundwater fraction will be smaller for all these cases with or without abstraction or infiltration then for the reference case.

5.2 Changes in phreatic groundwater levels

Variations of phreatic groundwater levels in some polder areas -with *controlled polder levels*- influence groundwater flow in the geohydrologic system and seepage through the Holocene aquitard. Together with seepage, also chloride load in the polder area changes. These changes are local at those polder areas where phreatic groundwater levels are varied.

Fig. 18 shows changes in volume distribution of fresh, brackish and saline groundwater for the next millennium due to variations in phreatic groundwater level. As can be seen, the differences may be significantly, depending on the magnitude of the phreatic groundwater level and the area over which the elevation is present. For instance, for an elevation of the phreatic groundwater level to the original phreatic groundwater level over all polders (to about 0.0 m *N.A.P.*), the changes in volume distribution of groundwater are relative small compared to the reference case, since such a elevation of phreatic groundwater level reduces the groundwater flows extremely. However, the question is how realistic these supposed compensating human measures are.

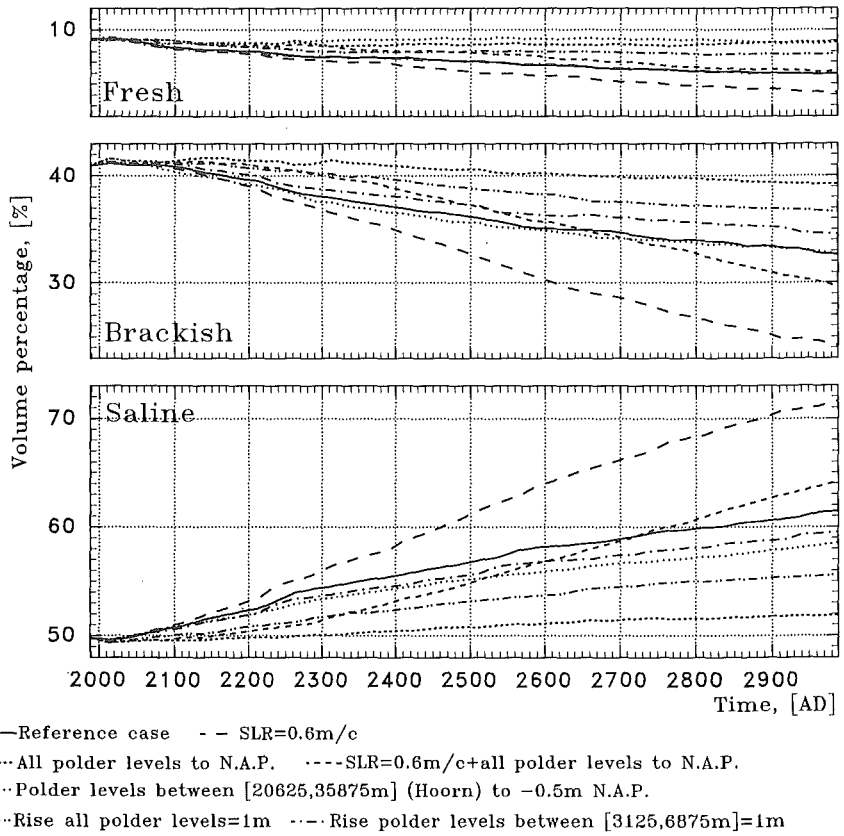

Figure 18: *The volume percentages of fresh, brackish and saline groundwater in the geohydrologic system. A comparison between different elevations of phreatic groundwater levels.*

6. PARAMETER ANALYSIS

Finally, some geohydrological parameters, which exact values are uncertain and which influence the simulation of the geohydrologic system significantly, are analysed.

(a) Longitudinal dispersivity α_L.

The chloride distributions after 500 years are given in fig. 19 for the reference case, but now for four different longitudinal dispersivities: α_L is 0.021 m[9] (reference case), 0.21 m, 2.1 m and 21.0 m. Looking at the position of the isochlor 16000 $mg\ Cl^-/l$, the figure shows that there is no salt water intrusion for the two cases with large longitudinal dispersivities, which

[9]As MOC uses the Anglo-Saxon system, α_L equals 0.07 feet in the reference case.

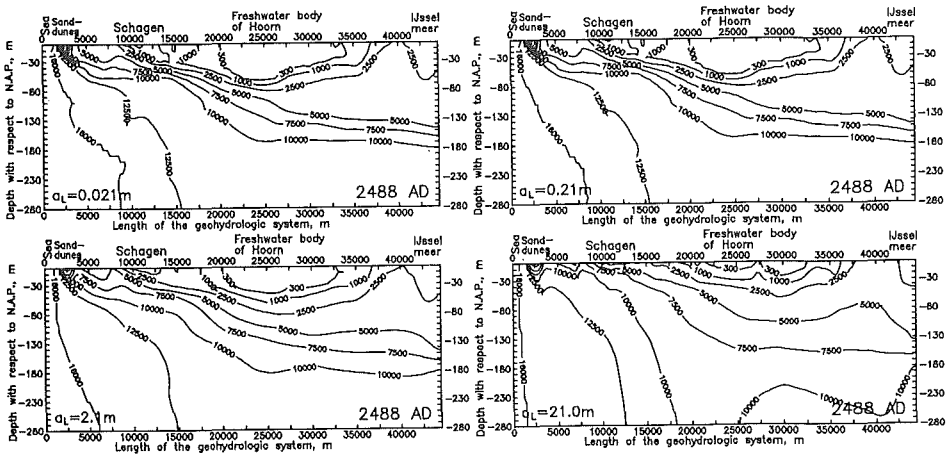

Figure 19: *The chloride distribution in the year 2488, calculated with four different longitudinal dispersivities: α_L: 0.021 m (reference case), 0.21 m, 2.1 m and 21.0 m.*

is unlikely to be expected according to the inland groundwater flow at the seaside boundary. Meanwhile, the two cases with relative small longitudinal dispersivities closely correspond with each other. Furthermore, the case with α_L equal to 21.0 m shows that the fresh waterbody at Hoorn is disappeared and that the geohydrologic system consists only a large zone with brackish groundwater. This conclusion is also founded by the volume distributions of the geohydrologic system -not shown here-: if α_L is 21.0 m, about 20 % of the fraction saline groundwater is transformed into brackish groundwater for the next millennium.

(b) Hydraulic conductivity of the geohydrologic system.
Obviously, the magnitude of hydraulic conductivity of aquifers is quite important for groundwater flow through geohydrologic systems. In fig. 20, the volume distributions in percentages are shown for several multipliers of the hydraulic conductivity, used in the reference case. The figure shows that the influence of the hydraulic conductivity is significant. This is especially due to the fact that the deep aquifers have high transmissibilities that cause rapid salt water intrusion. The influence on the volume distributions of the anisotropy factor (k_{vert}/k_{hor} up to 0.25 -not shown here-) seems to be relative small (a few percents differences).

(c) Porosity.
Porosities, from 0.35 up to 0.5, also seem to have relative small influences on the volume distributions. However, when the porosity is smaller then 0.35 (of the reference case), the volume distribution can be different significantly, as can be seen for p=0.15 in fig. 20.

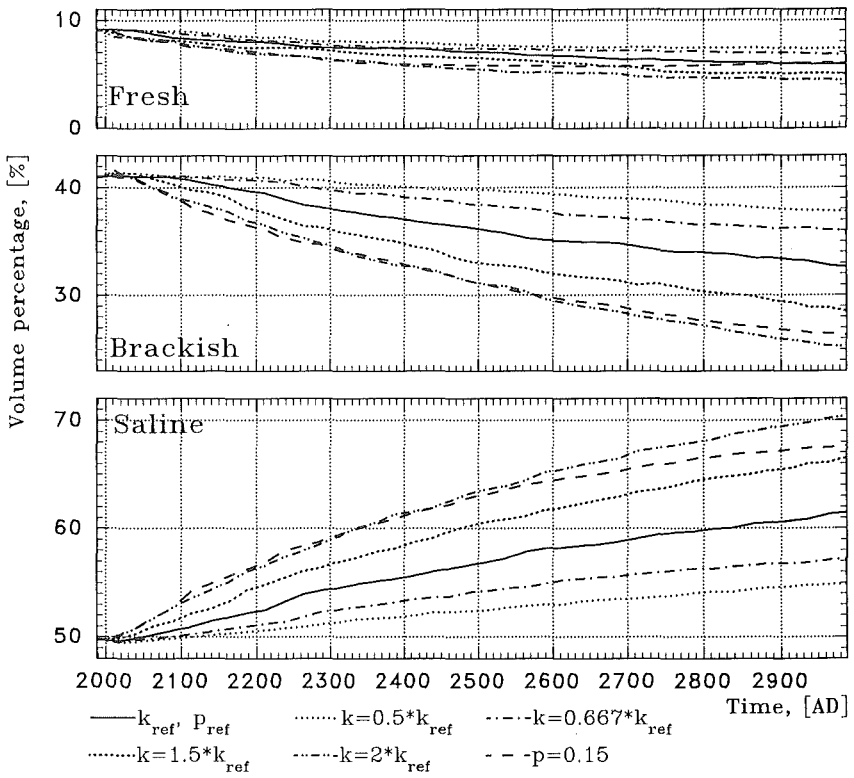

Figure 20: *The volume percentages of fresh, brackish and saline groundwater during the next millennium for several multipliers of hydraulic conductivity: 1.0*ref (reference case); 0.5*ref; 0.667*ref, 1.5*ref and 2*ref; and for the porosity equal to 0.15.*

CONCLUSIONS

Human interventions dominate groundwater flow in the cross-section of the studied area. The reclamation of polders has generated a strong saline groundwater flow from the sea through the deeper aquifers: the salt water intrusion. Nevertheless, salinisation proceeds slowly.

However, sea level rise accelerates salinisation significantly. Salt water intrusion will extend several kilometres more inland, because of high transmissibilities in the deeper aquifer. As a result, changes in quality and quantity of seepage in the polders near sea can not be neglected. However, a considerable time lag of several centuries occurs between the causes of changes and the ultimate effects on the salinisation process. The shallow aquifer (between

-20 and -30 m *N.A.P.*) and aquitards will contain only saline groundwater. The seepage in the polders in the first 15 kilometres from the coastline will increase significantly after some centuries and will contain much more saline groundwater.

If no sea level rise occurs, the fresh waterbody of Hoorn would remain. However, if a sea level rise of 0.6 m per century -as generally accepted- occurs, the fresh waterbody will decrease.

Human interventions may compensate the effect of sea level rise. Abstractions of saline groundwater or deep-well infiltrations of surface water may enlarge and create freshwater lenses. Both human measures may diminish chloride load through the Holocene aquitard. However, even with these compensating human measures, it takes a considerable time lag (several centuries) before changes in the fraction of fresh, brackish and saline groundwater and in the solute distribution of seepage are significant.

Even so, the effects of sea level rise on salinisation may be in the same order of magnitude as possible errors in geohydrological parameters, such as transmissibilities and hydrodynamic dispersion. The longitudinal dispersivity α_L, as used in MOC, must be set to a small value (in the order of centimetres or decimetres) so that the simulated solute distribution corresponds to the observations.

In this study, the conditions of aquitards remain constant. However, research has indicated that especially such layers may react chemically on changes of solutes in groundwater, especially of the chloride-ion (Goldenberg, *et al.*) [18]. Thus, the hydraulic conductivity of these layers should be adapted for changes in solute content of passing groundwater.

Acknowledgement

The authors wish to thank L.C. Lebbe of the Laboratory of Applied Geology and Hydrology of the State University of Ghent and J.P. van der Eem of the Testing and Research Institute of The Netherlands waterworks KIWA for their release of postprocessors and documentation that made it possible to adapt MOC for density differences. This study is performed with support from Delft Hydraulics.

References

[1] SCHULTZ, E. - *"Water Management of the Drained Lakes in The Netherlands"*. Ph.D.-thesis. (in Dutch). ISBN 90-369-1087-0. Rijkswaterstaat, Directie Flevoland. Lelystad, 1992.

[2] Instituut voor Cultuurtechniek en Waterhuishouding (ICW). Wageningen. *"Kwantiteit en kwaliteit van grond- en oppervlaktewater in Noord-Holland benoorden het IJ."* (in Dutch). Werkgroep Noord-Holland. ICW Regionale Studies 16, pp. 166, 1982.

[3] BEEKMAN, H.E. - *"Ion Chromatography of Fresh- and Seawater Intrusion." Multicomponent dispersive and diffusive transport in groundwater.* Ph.D.-thesis. ISBN 90-900 709-3. Drukkerij Fedo B.V. Enschede, 1991.

[4] POMPER, A.B. - Observations on the hydrochemical groundwater situation of the western Netherlands. *Geologie en Mijnbouw,* **62**, *585-592 (1983).*

[5] PAAP, H.A. - De invloed van de stijging van de zeespiegel op het verziltingsproces. Het model Konikow-Bredehoeft toegepast op een doorsnede in Noord-Holland. (in Dutch). *Master thesis at the Delft University of Technology, pp. 139, 1992.*

[6] WILDE, DE, J.G.S. - Begrenzing, oppervlakte, afvoer and peilen van de polders in Noord-Holland ten Noorden van het IJ an het Noordzeekanaal. (in Dutch). Werkgroep Noord-Holland IX. *Nota ICW 1160. Wageningen. pp. 13, (1979).*

[7] POMPER, A.B. - Geohydrological situation of the western part of The Netherlands. *Geologie en Mijnbouw,* **62,** *3/4, 519-528 (1983).*

[8] WITT, H. - Het chloridegehalte van het grondwater in Noord-Holland benoorden het IJ en het Noordzeekanaal. (in Dutch). Werkgroep Noord-Holland X. *Nota ICW 1173. Wageningen. pp. 25, (1980).*

[9] LAGEMAN R. and HOMAN, M. - Grondwaterkaart van Nederland, Alkmaar (19 west, 19 oost en 20A) en Medemblik (14 west, 14 oost). (in Dutch). *The TNO Institute of Applied Geoscience Delft. pp. 70, (1979).*

[10] KONIKOW, L.F. and BREDEHOEFT, J.D. - Computer model of two-dimensional solute transport and dispersion in ground water. *U.S. Geological Survey Techniques of Water-Resources Investigations, Book 7, Chapter C2, pp. 90, 1978.*

[11] MOC: Computer Model of Two Dimensional Solute Transport and Dispersion in Ground Water. *International Ground Water Modeling Center, Delft, Version 3.0, november 1989.*

[12] LEBBE, L.C. - The subterranean flow of fresh and salt water underneath the western Belgian Beach. *Proceedings of the 7th Salt Water Intrusion Meeting, Uppsala. Sver. Geolog. Unders. Rap. Meddel.,* **27,** *193-219, 1981.*

[13] LEBBE, L.C. - Mathematical model of the evolution of the fresh water lens under the dunes and beach with semi-diurnal tides. *Proceedings of the 8th Salt Water Intrusion Meeting, Bari. Geologia Applicata e Idrogeologia. vol. XVIII, Parte II, 211-238, 1983.*

[14] EEM, VAN DER, J.P. - Aanpassing Konikow-Bredehoeft voor Dichtheidsverschillen. (in Dutch). *Interne notitie KIWA. Augustus 1987.*

[15] OUDE ESSINK, G.H.P. - A sensitivity analysis of the adapted groundwater flow model MOC of Konikow & Bredehoeft. *Proceedings of the 12th Salt Water Intrusion Meeting, Barcelona, Spain. 1992.*

[16] STUYFZAND, P.J. - Hydrochemie en hydrologie van duinen en aangrenzende polders tussen Noordwijk en Zandvoort aan Zee (kaartbladen 24H en 25C). (in Dutch). *KIWA SWE-87.007, pp. 343, 1988.*

[17] KOOIMAN, J.W. - Modelling the salt-water intrusion in the dune water-catchment area of the Amsterdam Waterworks. *Proceedings of the 10th Salt Water Intrusion Meeting, Ghent, 1988.*

[18] GOLDENBERG, L.C., MANDEL, S. and MAGARITZ, M. - Fluctuating, non-homogeneous changes of hydraulic conductivity in porous media. *Quarterly Journal of Engineering Geology, London, Vol.* **19,** *pp. 183-190. 1986.*